Crystal growth, Structure and Characterization of NLO active Strontium Dihydrogen Diphthalate

R. Markkandan[*1,2], S.Sivaraman,[1]
[1]Department of Chemistry, Annamalai University, Chidambaram, India
[2]Department of Chemistry, Thiru.A.Govindasamy Government Arts College, Tindivanam, India

Abstract : Single crystals of strontium dihydrogen diphthalate (SDP) were grown by the slow evaporation solution growth technique. The structure is elucidated by single-crystal X-ray diffraction analysis and the crystal belongs to an orthorhombic system with noncentrosymmetric space group Cmc21. The cell parameters are, a = 28.400(10)Å,b = 8.758(3)Å, c = 6.953(2)Å, V = 1729.55(10)Å and Z = 4. The functional groups present in the molecule are identified by FT-IR stretching and bending frequencies. The structure and the crystallinity of the material were confirmed by powder X-ray diffraction analysis and the simulated X-ray diffraction (XRD) closely matches the experimental one with varied intensity patterns. The scanning electron microscopy study reveals the surface morphology of the grown crystal. The presence of Sr(II) in the specimen is confirmed by the Energy dispersive X-ray spectroscopy. The experimental band gap energy is estimated by the application of the Kubelka–Munk algorithm and the theoretical energy is determined by electronic band structure. The calculated band structure and the density of states of SDP suggest that its direct band gap energy is 3.95 eV, showing a reasonable agreement with the experimental value. Electronic structure is probed by first-principle study, carried out using the structural parameters of the single crystal. The investigation of the intermolecular interactions and crystal packing via Hirshfeld surface analysis, based on single-crystal XRD, reveals that the close contacts are associated with molecular interactions. The relative second harmonic generation (SHG) efficiency measurements reveal that efficiency of SDP is comparable to that of KDP.

***Keywords*–Second harmonic generation, Hirshfeld surface analysis, Band structure**

I. INTRODUCTION

Potassium hydrogen phthalate (KHP) is well known for its application in the production of crystal analyzer for long wave X-ray spectrometer [1-2]. KHP possesses piezoelectric, pyroelectric, elastic and nonlinear optical properties [3-5]. It crystallizes in orthorhombic system with space group $Pca2_1$ [6]. It has platelet morphology with perfect cleavages along (010) plane. Recently, KHP crystals are used as substrates for the growth of highly oriented film of conjugated polymers with nonlinear optical susceptibility [7-8]. It is used as a substrate for the deposition of thin films of NLO materials like urea with high mechanical stability [9]. Hottenhuis et al [10]. have made detailed investigations on the surface morphology and the growth kinetics of the KHP (010) face.

The optical, dielectric, thermal properties [11] and structure [12] of lithium hydrogen phthalate have been investigated. It was observed that the second harmonic generation (SHG) efficiency of sodium hydrogen phthalate is double that of KHP crystals [13]. Single crystals of $Sr(C_8H_5O_4)_2.2H_2O$ were grown from an aqueous solution of $SrCO_3$ and an excess of phthalic acid[14]. Structure of cesium (I) hydrogen phthalate reveals that Cs^+ cation is surrounded by eight O atoms [15] while Mg^{2+} cation is octahedrally coordinated in hexaaquamagnesium hydrogen phthalate [16]. Manganese dihydrogen diphthalate dihydrate crystallizes in the monoclinic space group $P21/c$ [17]. The structures of $[Co(H_2O)_6](C_8H_5O_4)_2$[18-19] and $NiH_2(C_8O_4H_4)_2.6H_2O$ [20] consist of octahedrally coordinated cations. Influence of alkaline cation on the structure of polymeric *o*-phthalatocuprate(II) has been studied [21]. Molecular structures of magnesium di-*o*-phthalatocuprate (II) dihydrate and strontium di-*o*-phthalatocuprate(II) trihydrate [22] crystals consist of *o*-phthalatocuprate(II) complexes, joined in linear polymeric chains by bridging *o*-phthalate anions of alkaline-earth cations and of water molecules. Polymeric dihydroxydiphthalatotricobalt(II) crystallizes in orthorhombic space group *P*ccn[23]. Molecular structures of $K_2[Ni(H_2O)_6](C_8H_5O_4)_4\cdot 4H_2O$[24] and $K_2[Co(H_2O)_6](C_8H_5O_4)_4\cdot 4H_2O$ have been reported[25].

Recently, we have investigated the influence of rare earth, alkaline earth and transition metal doping on the properties and crystalline perfection of KHP crystals [26-27]. Accommodating capability of KHP crystals with dopants Os(VIII)[28], Zn(II)[29] and Na(I)[30] reveal some interesting features. Growth, crystalline perfection and characterization of Ni(II)[31], Co(II)[32] and Na(I)[33] incorporated aqua complexes of KHP have been reported. Synthesis, structural aspects and NLO activity of KNaP[34] and lithium potassium hydrogen phthalate[35] mixed crystals also reported recently. Growth, structure and characterization of nickel(II) doped hexaaqua cobalt(II) dipotassium tetrahydrogentetraophthalate tetrahydrate was reported[36]. As the part of our investigation in the study of phthalate crystals, here we report the crystal growth, structure, characterization, computational studies and nonlinear optical properties of strontium dihydrogen diphthalate [SDP].

II. Experimental

Synthesis

SDP was synthesized from an aqueous solution of AR grade $SrCl_2$ and potassium hydrogen phthalate (Merk) taken in a stoichiometric ratio of 1:2. This mixture was stirred for 3 h by a magnetic stirrer. Crystals from aqueous solution were grown by slow evaporation solution growth technique at room temperature. The beaker containing solution was tightly covered with a thin polythene sheet to control the evaporation rate of the solvent and kept undisturbed in a dust free environment. The crystals were harvested after 5-8 d. As-grown SDP crystal is shown in Fig.1.

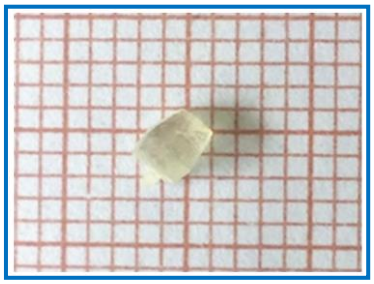

Fig.1Photo images of as–grown SDP crystals

Computational studies

Energy calculation, hyperpolarizability and Mulliken atomic charges were performed using the *GAUSSIAN 09W* program package on a personal computer without any constraints on the geometry using density functional group theory (DFT) B3LYP method with LanL2DZ as the basis set. By the use of the *GAUSSVIEW* 5.0 molecular visualization program the optimized structure of the molecule has been visualized. Hirshfeld surfaces and fingerprint plots were generated by crystal explorer program. Band structure and density of states were calculated by virtual nano program based on density functional theory (DFT). A kinetic energy cut-off of 500 eV and the Monkhorst–Pack K point mesh of 4 x 4 x 8 were chosen for HT phases. The energy cut-off of the plane wave basis set was 300 eV.

III. Results and discussion

3.1 FT-IR

The FT-IR spectrum of the as-grown specimen is shown in Fig.2.An absorption band in the region 500-900 cm^{-1} is due to C-H out of plane deformations of aromatic ring. The C=O stretching frequency appears at 1668 $cm.^{-1}$ The O-H frequency appears at 3472 cm^{-1} and O-C=O frequency at 1562 cm^{-1} and the O-H-O frequency appeared at 1154 $cm.^{-1}$ FT-IR frequencies of SDP and KHP are shown in Table 1.

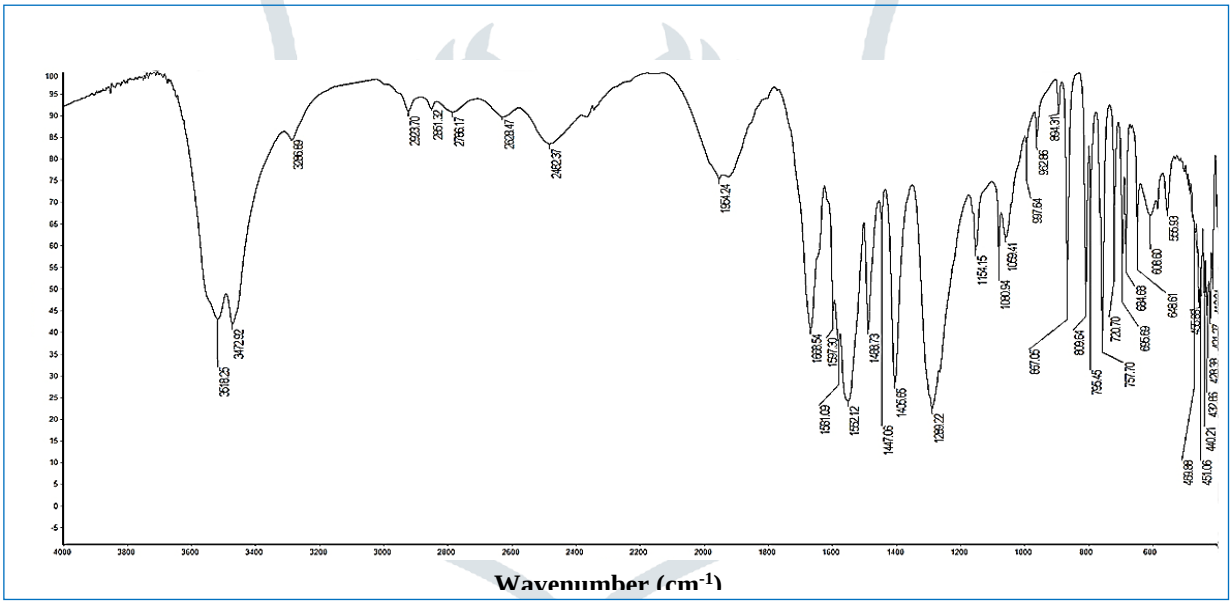

Fig.2 FT-IR spectrum of SDP

Table 1 Observed vibrational bands of SDP (cm^{-1})

KHP	SDP	Frequencies(cm^{-1})
1078	1080	v_{as}O-H-O
1144	1154	v_s(O-H-O)
1445	1405	v_{as}O-C=O
1565	1562	v_sO-C=O
1675	1668	v_s(C=O)
3470	3472	v_s(O-H)

3.2 Powder XRD analysis

The powder XRD of SDP shows that the sample is of a single phase without any detectable impurity. The well-defined Bragg peaks at specific 2ɵ angles show good crystallinity of the specimen. Not much variation are observed in the peak positions of powder and simulated XRD patterns (Fig.3).However, the relative intensities differ and this could be due to the preferred orientation of the sample used for diffractogram measurement. Also, the mosaic spread of powder and single crystal patterns differ, resulting in intensity variations. High intensity sharp peaks show good crystalline nature.

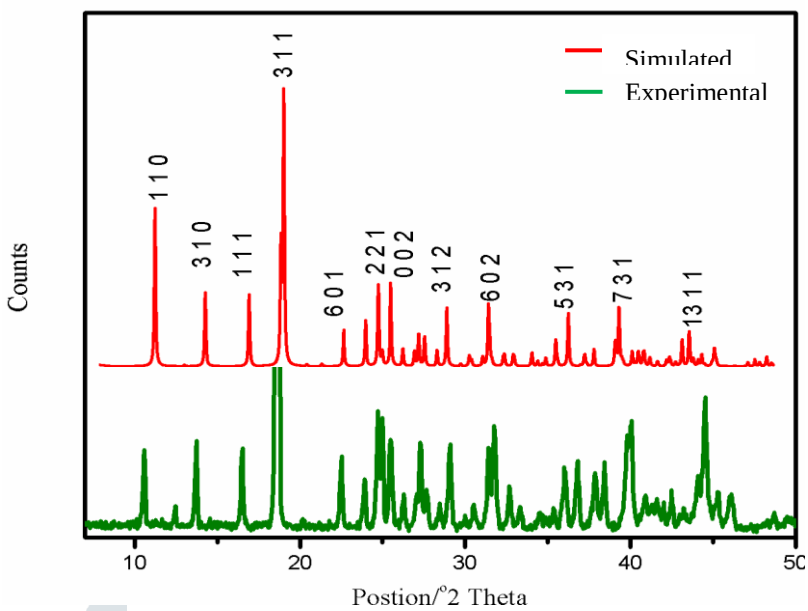

Fig.3 Powder XRD Pattern

3.3 Single crystal XRD

The structural analysis of SDP was carried out by single crystal XRD analysis. An ORTEP view, Optimized molecular structure and packing diagram of SDP is given in Fig.4and it crystallizes in an orthorhombic system with noncentrosymmetric space group $Cmc2_1$. The cell parameter values are in (Table 2) agreement with already reported values of $Sr(C_8H_5O_4).2H_2O$ obtained from an aqueous solution of $SrCO_3$ an excess of phthalic acid[14]. The structure refinement covered at R1 = 0.0172 and wR2=0.0390. The chemical formula $C_{16}H_{14}O_{10}Sr$ confirms the presence of Sr in the crystalline matrix, well supported by EDS. Strontium metal is coordinated by two phthalate ligands through their oxygen atoms with Sr-O bond angles ranging from 152.78(7) to 158.31(7) Å. The hydrogen phthalate proton is involved in a relatively strong intermolecular hydrogen bond (Table 3).However, no short intramolecular hydrogen bond exists.

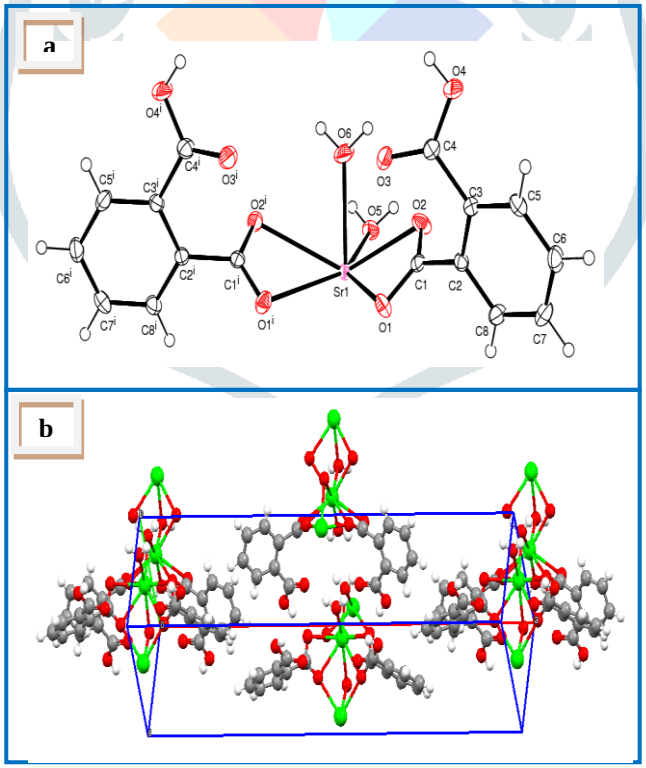

Fig.4 (a) ORTEP (b) Packing diagram of SDP

The benzene ring is planar and has an average C-C distance of 1.501Å. The average C-H distance and C-C-H angle are 0.9300 and 119.6Å respectively. O(6) has an exceptionally large thermal parameter in the z direction (U^{33} = 0.228Å^2), indicating possible disorder. O(1) hydrogen bond, this effect is partly reflected in the thermal parameters of O(1), and is also apparent for O(2). Refinement with a statistical distribution of O (6) indicated disorder of this atom to be significant. However, because of large correlations, only the average position of O(6) is reported here; the disorder was found to have a minimal effect on the intermolecular distances. The selected hydrogen bond lengths are given in Table 3.Weak intermolecular interactions are observed for O(4)-H(4)···O(2)5, O(6)-H(6A)···O(3)6 and, O(5)-H(5A)···O(3)7 with bond distances of 1.73, 1.95(2) and 2.10(2) Å respectively. General observation is, when the specimens crystallize in an orthorhombic system they opt for a noncentrosymmetric space group whereas when they crystallize in monoclinic system they prefer centrosymmetric space group.

It appears that the foreign metal induces nonlinearity by enhancing the charge transfer.

Table 2 Crystal data of some metal phthalates

M	a(Å)	b (Å)	c (Å)	Z	System	Space group	Symmetry	Reference
Na^+	6.76	9.31	26.42	8	Orthorhombic	B2ab	-	37
Cs^+	10.659(5)	12.768(6)	6.356(3)	4	Orthorhombic	$Pca2_1$	Noncentrosymmetry	37
NH_4^+	6.40	10.23	26.14	8	Orthorhombic	Pcab	-	37
$CH_3NH_3^+$	7.22	11.01	24.46	8	Orthorhombic	Pcab	-	37
K^+	6.47	9.61	13.26	4	Orthorhombic	$P2_12_12$	Noncentrosymmetry	6
Rb^+	6.55	10.02	12.99	4	Orthorhombic	$P2_12_12$	Noncentrosymmetry	37
Tl^+	6.63	10.54	12.95	4	Orthorhombic	$P2_12_12$	Noncentrosymmetry	37
Cs^+	6.58	10.81	12.84	4	Orthorhombic	$P2_12_12$	Noncentrosymmetry	15
Li^+	16.837(2)	6.822(1)	8.198(2)	4	Orthorhombic	Pnma	Centrosymmetry	12
Sr^{2+}	28.400(10)	8.7585(3)	6.953(2)	4	Orthorhombic	$Cmc2_1$	Noncentrosymmetry	present work
Ni^{2+}	16.024(2)	16.024(2)	12.500(2)	4	Monoclinic	$P2_1/C$	Centrosymmetry	20
Co^{2+}	6.560(1)	30.962(4)	9.918(1)	4	Monoclinic	$P2_1/C$	Centrosymmetry	18
Mn^{2+}	13.018(6)	5.518(1)	12.940(3)	2	Monoclinic	$P2_1/C$	Centrosymmetry	17
Cu^{2+}	8.31(2)	14.62(2)	7.20(2)	2	Monoclinic	$P2_1/C$	Centrosymmetry	22
Mg^{2+}	6.565(1)	30.840(4)	10.005(1)	4	Monoclinic	$P-_1$	Centrosymmetry	16

Table 3 Hydrogen bonds for SDP [Å].

D-H···A	d(D-H)	d(H···A)	d(D···A)	<(DHA)
O(4)-H(4) ···· O(2)#5	0.82	1.73	2.546(3)	170.0
O(6)-H(6A) ···· O(3)#6	0.85(2)	1.95(2)	2.794(3)	175(5)
O(5)-H(5A) ···· O(3)#7	0.82(2)	2.10(2)	2.914(3)	176(4)

Symmetry transformations used to generate equivalent atoms:
#1 -x+1,-y, z+1/2 #2 -x+1,-y,z-1/2 #3 x,-y,z-1/2
#4 -x+1, y,z #5 x,-y+1,z+1/2 #6 -x+1,-y+1,z-1/2

3.4 SEM

SEM study gives information about the surface morphology. The SEM pictures of SDP crystals at different magnifications are given in Fig.S4exposing the surface roughness due to bunched steps or macro steps formation in a plate like morphology. The presence of strontium in the doped specimen was confirmed by EDS Fig.5.

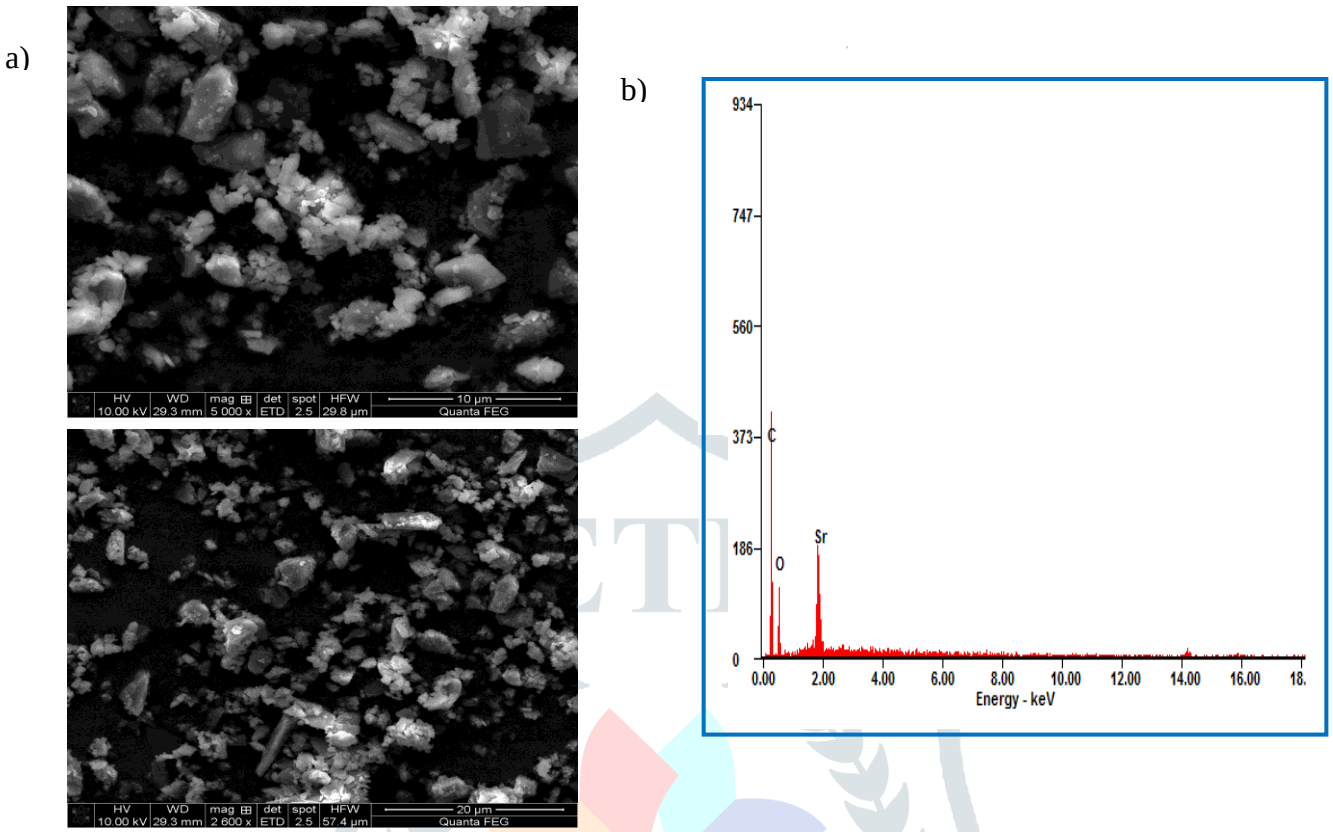

Fig.5 a) SEM b) EDS image of SDP

3.6 UV-Vis-NIR diffuse reflectance spectrum

The concentration of an absorbing species can be determined using the Kubelka–Munk algorithm correlating reflectance and concentration,

$$F(R) = (1-R)^2/2R = \alpha/s = Ac/s$$

where F(R) is the Kubelka-Munk function, R is the reflectance of the crystal, α is the absorption coefficient and s is the scattering coefficient, A is the absorbance and c is the concentration of the absorbing species. The optical absorption spectrum shows that the absorption is minimum in the visible region and the cut-off wavelength is ~290 nm. The direct band gap energy of the specimen is estimated as 4.11 eV from the Tauc plot $[F(R)hv]^2$ versus hv(eV)(Fig.6).

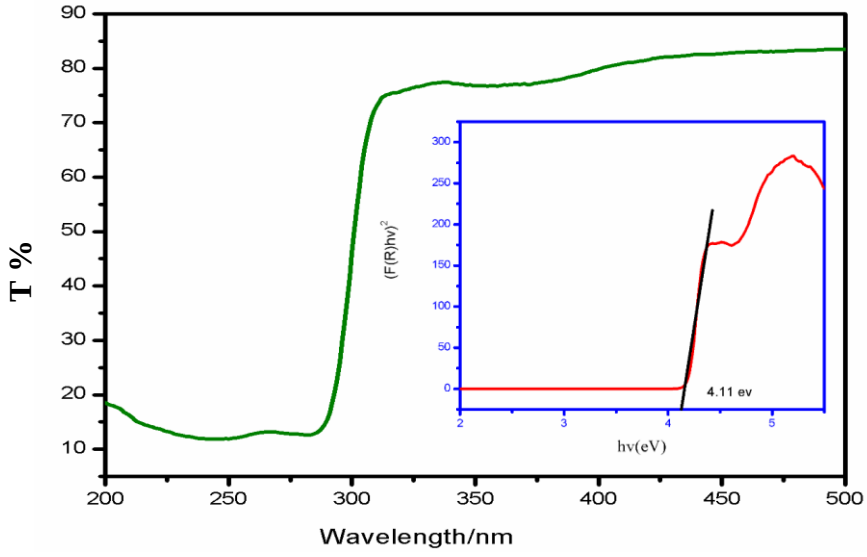

Fig.6 UV- vis spectrum of SDP (Tauc plot is given as an inset)

3.7 Band structure and density of states

States close to the band gap mainly determine the optical properties of a crystal in the UV-vis spectra[38](Fig. 4a).The calculated band structure along the lines of high symmetry points in the Brillouin zone of SDP is shown in Fig. 7a and b,The Brilloiuin zone of SDP, displays the dispersion of the bands along the high symmetry k-points defined in units of the reciprocal lattice vectors. The optimized norm-conserving pseudo potential [39] in the Kleinman–Bylander[40] form allows us to use a relatively small basis set without compromising the computational accuracy, and the Sr: $4s_2\ 4p_6\ 5s_2$, O: $2s_2\ 2p_4$ are treated as the valence electrons. Our tests showed that the computational parameters above are accurate enough for the present purpose. It is shown that SDP is a direct gap compound with a calculated band gap of 3.95 eV (Fig. 4a).It agrees well with the experimentally determined value of 4.11 eV and the small difference is attributed to the discontinuity in the derivative of the exchange-correlation energy within density functional theory (DFT) [41].

The nature of chemical bonding can be elucidated from the total and partial density of states (DOS) and further evidenced by Mulliken population analysis. The total and partial DOS analyses shown in Fig.8 indicate that the O-2*p* states provide the significant contributions to the tops of VBs from 2.78 eV to the Fermi level. The O-2*p* and O-2s states produce the VBs from 0 eV to −11 eV and -18 eV to -22 eV above the Fermi level. The CBs from 15.62 eV to 25.0 eV and 0.3eV to -10 eV is chiefly derived from the unoccupied Sr-4p and Sr- 5s states, which means that the Sr atoms act primarily as electron donors. Similarly, the O atoms act as electron acceptors because their P states are localized below E_F. Since the optical properties are determined by the electron transition among the top of valence band and the bottom of the conduction band, the overlap found in the regions nearby Fermi level implies that they may play an important role in their optical properties [42].

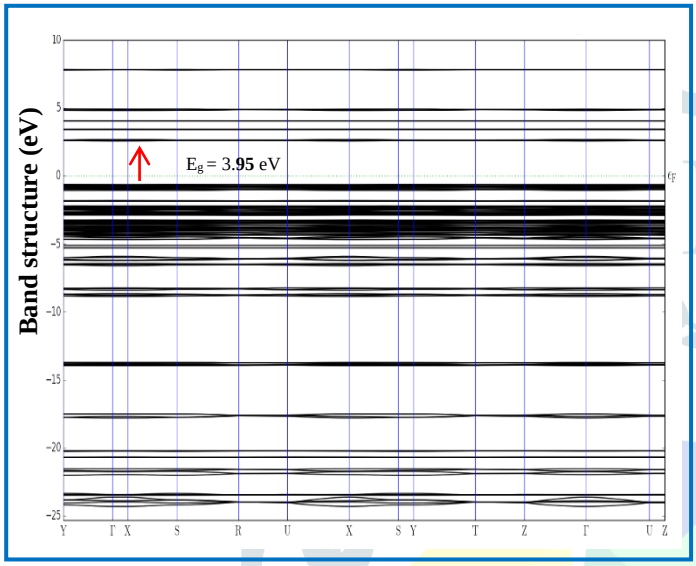

Fig.7 (a) Calculated Band structure of SDP

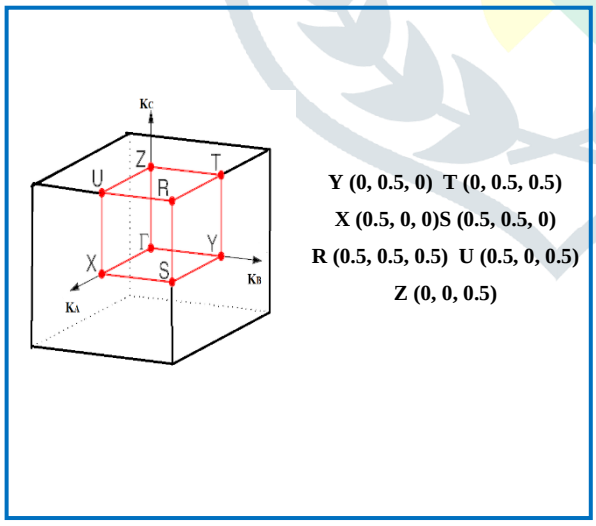

Fig.7 (b) The Brillouin zone of SDP

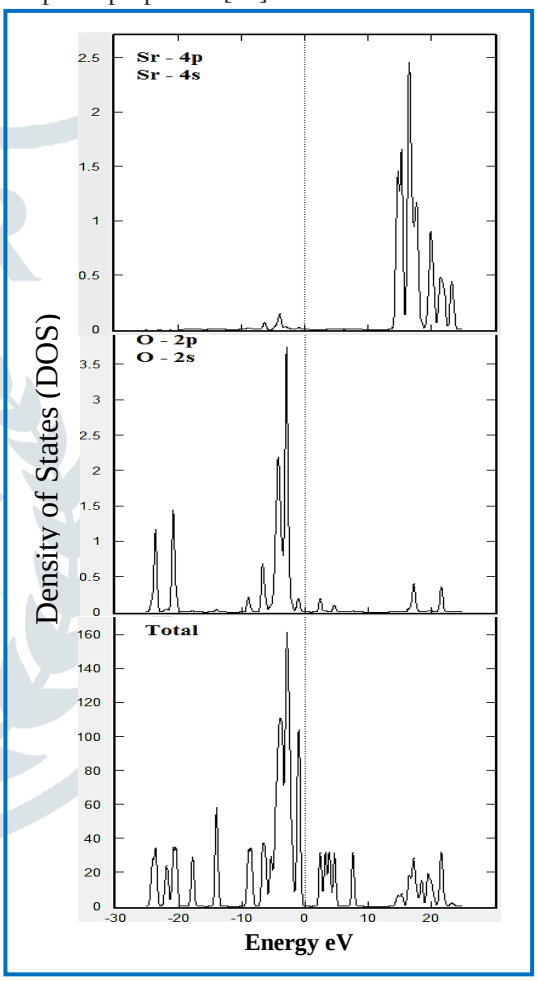

Fig.8 Total and partial density of states of SDP

3.8 SHG efficiency

The SHG test was performed by an Nd:YAG laser with a modulated radiation of 1064 nm, used as an optical source and directed on the powder sample through a filter with an input beam energy of 0.9 mJ/pulse. KDP sample was used as reference material and the powder SHG efficiency of SDP was found to be equal to KDP ($I_{2\omega}$= 96 mV), under identical conditions.

3.9 First-order molecular hyperpolarizability

The high NLO efficiency of SDP at the molecular level is also confirmed by computational studies, and the calculated first-order molecular hyperpolarizability (β) of the specimen is, β_{total} = 0.135x10^{-30}esu, ~0.3 times that of urea with dipole moment, μ equal to 1.0263D (Table 4). The high hyperpolarizability is due to the nonzero values. High beta value is a required

property of an NLO material. High beta is associated with high charge transfer. It could be due to strong inter- and intramolecular hydrogen bonding interaction enhancing the hyperpolarizability significantly leading to nonlinearity.

Table 4 First - order molecular hyperpolaraizability(β) of SDP

First - order molecular hyperpolaraizability	
β_{xxx}	1.477
β_{xxy}	-1.064
β_{xyy}	1.135
β_{yyy}	-7.886
β_{xxz}	1.178
β_{xyz}	-2.999
β_{yyz}	1.514
β_{xzz}	3.115
β_{yxx}	-1.273
β_{zzz}	7.758
β_{total}	0.135×10^{-30}

3.10 Hirshfeld surface analysis

The Hirshfeld surfaces of SDP mapped over d_{norm} (front view) (b) d_{norm} (back view) d_e, d_i, shape index surface andcurvedness are depicted in Fig.6.The d_i represents the difference from the Hirshfeld surface to the nearest nucleus inside the surface and d_e is meant for outside the surface[43]. The mapped surfaces are shown as transparent in a similar orientation around which they were calculated. The Hirshfeld surface surrounding a molecule is distinct defined by points where the contribution to the electron density from the molecule of target is equal to the contribution from all the other molecules. The large circular depressions (deep red) which are visible on the d_i surfaces are an indicator of hydrogen-bonding contacts, and other visible spots are due to H···H contacts. The dominant H···O and O···H interactions are viewed in Hirshfeld surfaces by the bright red area in Fig.6. The small area and light color on the surface indicate weaker and longer contacts other than hydrogen bonds.

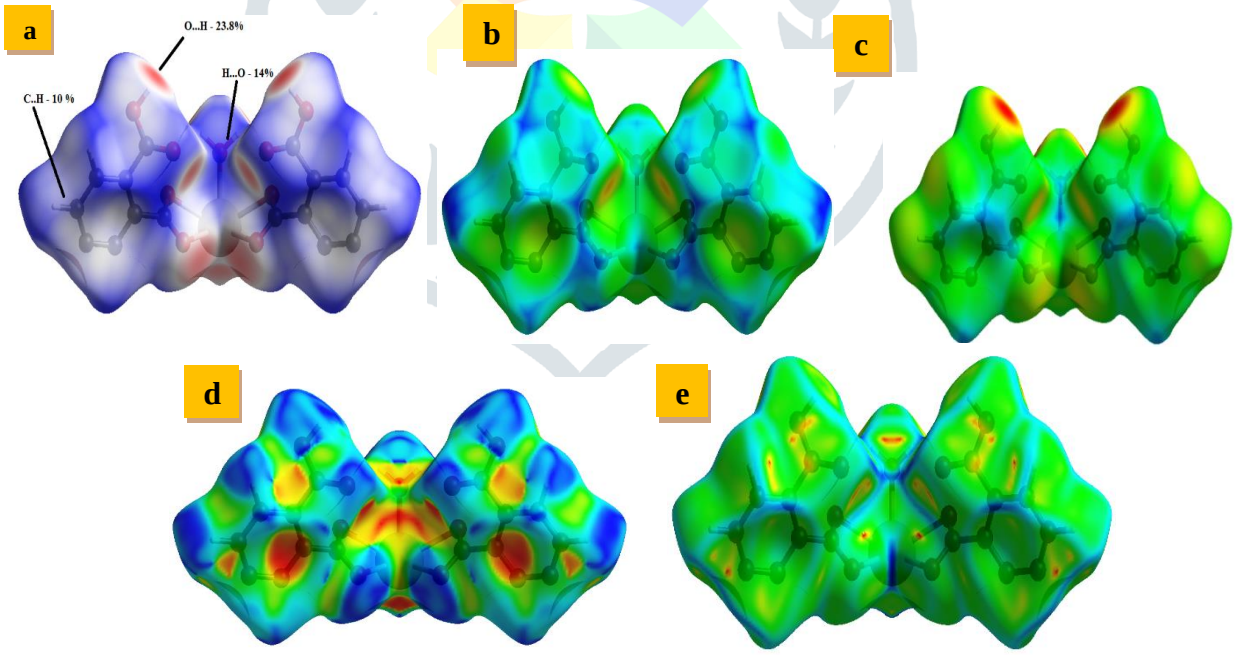

Fig.9 Hirshfeld surfaces of SDP (a) d_{norm} (b) d_e (c) d_i (d) Shape Index (e) Curvedness

3.11 Fingerprint analysis

The two-dimensional fingerprint plots of SDP clearly illustrate the intermolecular interactions pattern. These fingerprint plots are pretty asymmetric because the interactions take place connecting two chemically and crystallographically divergent molecules [44]. In the fingerprint region O···H (23.8 %) interactions are represented by a spike in the bottom area whereas the H···O (14 %) interactions are represented by a spike in the top left region in the fingerprint plot. Hydrogen bonding interactions H···H (23 %) are very high compared to the other bonding interactions.The finger print at the bottom right area represents C···H (10 %) interactions and top right area represents H···C (7.4 %) interactions. The fingerprint at the top center area represents C···C (1 %) interactions. The Relative contributions of various intermolecular interactions in SDP are shown in Fig.10.All the

interactions with percentages are given in a pie chart, Fig.11the molecular interactions can be differentiated: the strong interactions occupy more space and weak interactions occupy less space in the fingerprint plot.

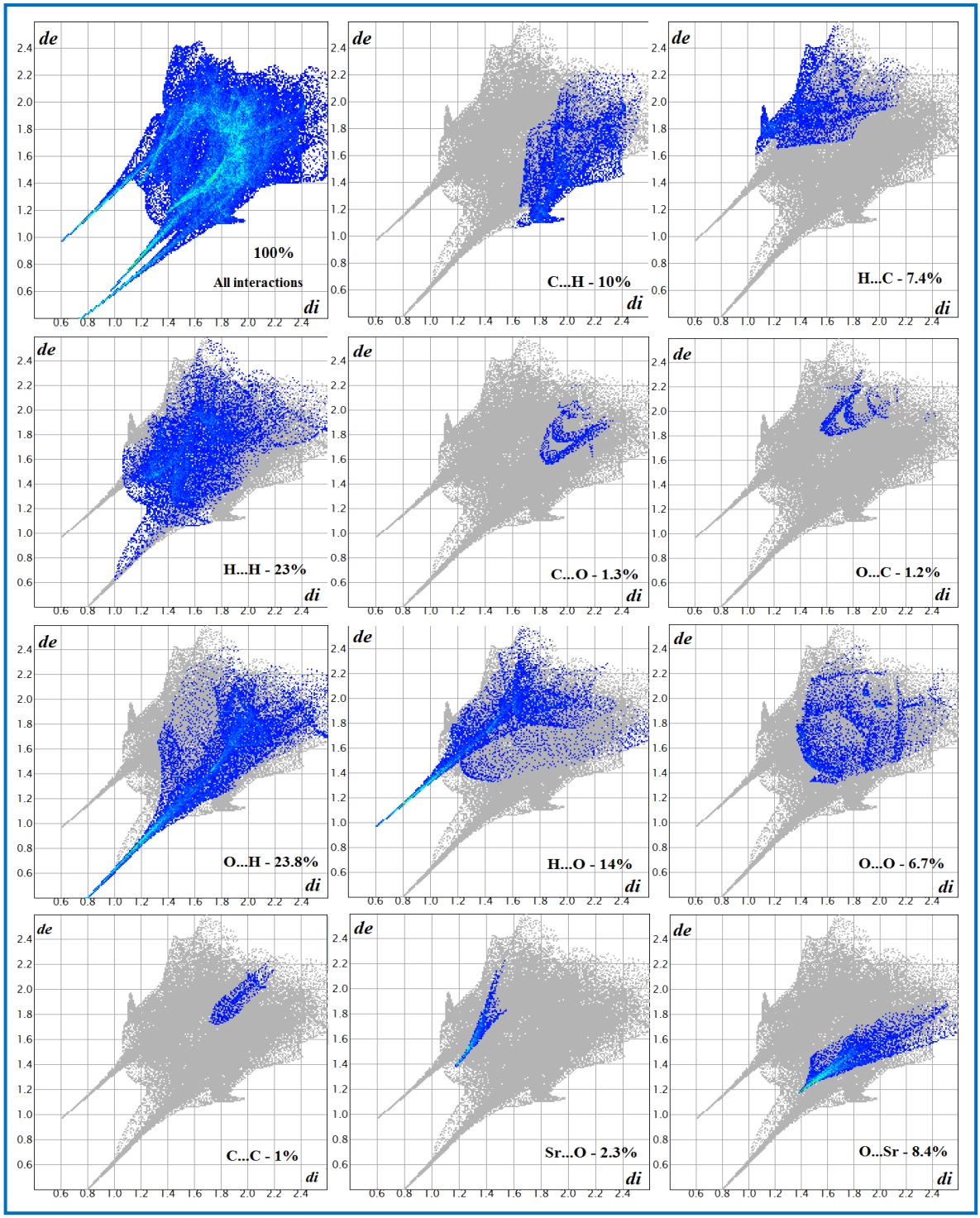

Fig.10 Fingerprint plots of SDP

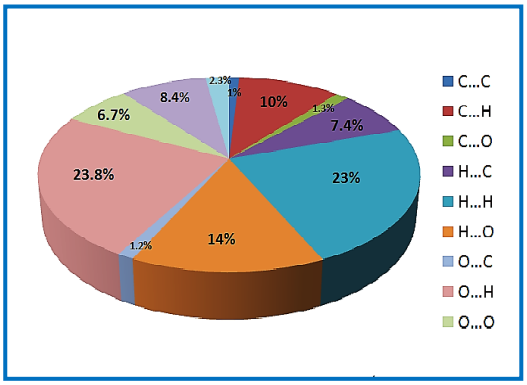

Fig.11 Quantities of molecular interactions represented in a pie chart

IV. Conclusions

Strontium dihydrogen diphthalate single crystals are grown by the slow evaporation solution growth technique. The crystal belongs to an orthorhombic system with noncentrosymmetric space group. The presence of strontium in the crystal was confirmed by EDS. The SEM image shows the surface morphology of the crystal. SDP exhibits a good SHG efficiency, optical transparency and reasonable thermal stability. Fingerprint plots of the Hirshfeld surfaces are used to locate and analyze the percentage of hydrogen bonding interactions. Dominant hydrogen bonding interactions such as O···H (23.8%) and H···O (14%) control the molecule orientations resulting is facile charge transfer. The intra- and intermolecular interactions are the prime factors responsible for charge transfer leading to nonlinearity as visualized by Hirshfeld surface analysis. Electronic band structure and density of states reveal a low band gap, associated with large β along with high SHG activity clearly evidence that SDP is a promising NLO material.

References

[1]Jones, J. L. Paschen, K. W and Nicholson, J. B. 1963. Performance of Curved Crystals in the Range 3 to 12 A.J. Appl. Opt, 2:955-961.

[2]Yoda, O. Miyashita, A. Murakami, K. Aoki, S. and N. Yamaguchi, 1991. Time-resolved x-ray absorption spectroscopy apparatus using laser plasma as an x-ray source. Proc. SPIE Int. Soc. Opt. Eng., 1503:463-466.

[3]Miniewicz, A and Bartkiewicz, S. 1993. On the electro-optic properties of single crystals of sodium, potassium and rubidium acid phthalates. Adv. Mater. Opt. Electr., 2:157-163.

[4] Kejalakshmy, N. and Srinivasan, K. 2004. Growth, optical and electro-optical characterization of potassium hydrogen phthalate crystals doped with Fe^{3+} and Cr^{3+} ions. Opt. Mater., 27: 389-394.

[5]Shankar, M. V and Varma, K. B. R. 1996. Piezoelectric resonance in KAP single crystals. Ferroelectrics Lett. Sec., 21:55-59.

[6]Okaya,Y. 1965. The Crystal Structure of Potassium Acid Phthalate, $KC_6H_4COOH.COO$, Acta Crytallogr., 19:879-882.

[7]Nisoli, M. Pruneri, V. Magni, V. De Silvestri, S. Dellepiane, G.Cuniberti, D. C and Le Moigne, J. 1994. Ultrafast exciton dynamics in highly oriented polydiacetylene films. Appl. Phys. Lett., 65:590-592.

[8]Timpanaro, S. Sassella, A. Borghesi, A. Porzio, W. Fountaine, P and Goldmann, M. 2001.Crystal Structure of Epitaxial Quaterthiophene Thin Films Grown on Potassium Acid Phthalate. Adv. Mater., 13:127-130

[9]Murugakoothan, P.Mohankumar, RUshashree, P. M. Jayavel, R. Dhanasekaran, R and Ramasamy, P. 1999. Habit modification of potassium acid phthalate (KAP) single crystals by impurities. J. Cryst. Growth., 207:325-329.

[10]Hottenhuis, M. H. J and Lucasius, C. B. 1989. The influence of internal crystal structure on surface morphology; in situ observations of potassium hydrogen phthalate{010}. J. Cryst. Growth., 94:708-720.

[11]Senthil, A. Ramasamy, P. Bhagavannarayana, G. 2009. Synthesis, growth, optical, dielectric and thermal studies of lithium hydrogen phthalate dihydrate crystal. J. Cryst. Growth., 311:2696–2701.

[12]W. Gonschorek, H. Kuppers, Acta Crystallogr. Sect. B: Struct. Sci., 1975, 31, 1068–1072.

[13]Bairava Ganesh, R. Kannan, V. Meera, K. Rajesh, N.P and Ramasamy, P. 2005. Synthesis, growth and characterization of a new nonlinear optical crystal sodium acid phthalate. J. Cryst. Growth., 282:429–433.

[14]Bats, J.W. Schuckmann, and W.Fuess, H.1978.Strontium dihydrogen diphthalate dehydrate. Acta Crystallogr. Sect. B: Struct. Sci., 34:2627–2628.

[15]Hu, M. Geng, C. Li, S. Liu, Z. Jiang, Y and Zhang,G. 2004. Caesium(I) hydrogen phthalate. Acta Crystallogr. Sect. E: Struct.Rep. Online., 60: 1713–1715.

[16] Kariuki, B.M and Jones, W. 1989. Structures of hexaaquamagnesium hydrogen phthalate and hexaaquamagnesium hydrogen phthalate dihydrate. Acta Crystallogr. Sect. C: Cryst. Struct. Commun., 45:1297–1299.

[17]Bats, J.W. Kallel, A and Fuess, H.1978. Structure of Manganese Dihydrogen Diphthalate Dihydrate. Acta Crystallogr. Sect. B: Struct. Sci., 34:1705–1707.

[18] Adiwidjaja, G.Rossmanith, E and Kuppers, H.1978. Cobalt dihydrogen diphthalate hexahydrate. Acta Crystallogr. Sect. B: Struct. Sci., 34:3079–3083.

[19]Kariuki, B.M and Jones, W.1993. Structure of Hexaaquacobalt Hydrogen Phthalate. Acta Crystallogr. Sect. C: Cryst. Struct. Commun., 49:2100–2102.

[20]Adiwidjaja, G and Kuppers, H. 1976. Nickel dihydrogen diphthalate hexahydrate. Acta Crystallogr. Sect. B: Struct. Sci., 32:1571–1574.

[21] Influence of the alkaline cation on the structures of polymeric o-phthalatocuprate(II). II. The crystal structures of disodium di-o-phthalatocuprate(II) dihydrate and dipotassium catena-di-μ-(o-phthalato)-cuprate(II)dehydrate. Acta Crystallogr. Sect. B: Struct. Sci., 34:412–416.

[22] BiaginiCingi, M. Lanfredi, A.M.M. Tiripicchio, A and Camellini, M.T. 1978., The crystal and molecular structures of magnesium di-o-phthalatocuprate(II) dihydrate and strontium di-o-phthalatocuprate(II) trihydrate. Acta Crystallogr.Sect. B: Struct. Sci., 1978, 34, 406–411.

[23]Yang, S.Y. Long, L.S. Huang, R.B. Zheng, L.S and Weng Ng,S.2003. Polymeric dihydroxydiphthalatotricobalt(II), Acta Crystallogr. Sect. C: Crystallogr. Struct. Commun., 59: 456–458.

[24]BiaginiCingi, M.Lanfredi, A.M.M and Tiripicchio, A.1984.Hexaaquaniekel(II) Dipotassium Tetrahydrogen Tetra-o-phthalate Tetrahydrate, $K_2[Ni(H_2O)_6][C_8H_5O_4].4H_2O$.Acta Crystallogr. Sect. C: Cryst. Struct. Commun., 40:56–58.

[25]N.G. Furmanova, T.A. Eremina, T.M. Okhrimenko, V.A. Kuznetsov, 2000. Crystal and molecular structures of potassium cobalt hydrogen phthalate $K_2[Co(H_2O)_6](C_8H_5O_4)_4.4H_2O$ and mechanism of Co^{2+} impurity trapping in KAP crystals. Crystallogr. Rep., 45:771–774.

[26]Kasthuri, L. Bhagavannarayana, G. Parthiban, S. Ramasamy, G. Muthu, K. and Meenakshisundaram,SP. 2010. Rare earth cerium doping effects in nonlinear optical materials: potassium hydrogen phthalate (KHP) and tris(thiourea)zinc(II) sulfate (ZTS). CrystEngComm., 12:493–499.

[27]Bhagavannarayana, G. Parthiban, S. Chandrasekaran, C and Meenakshisundaram,SP. 2009. Effect of alkaline earth and transition metals doping on the properties and crystalline perfection of potassium hydrogen phthalate (KHP) crystals. CrystEngComm, 11:1635–1641.

[28]Muthu, K. Bhagavannarayana, G. Chandrasekaran, C.Parthiban, S. S.P.Meenakshisundaram and Mojumdar.S.C. 2010. Os(VIII) doping effects on the properties and crystalline perfection of potassium hydrogen phthalate (KHP) crystals. J. Therm. Anal. Calorim., 100: 793–799.

[29] Parthiban, S. Murali, S.Madhurambal, G. Meenakshisundaram, S.P and Mojumdar.S.C. 2010.Effect of zinc(II) doping on thermal and optical properties of potassium hydrogen phthalate (KHP) crystals. J. Therm. Anal. Calorim., 100:751–756.

[30]Ramasamy, G. Parthiban, S. Meenakshisundaram, S.P and Mojumdar.S.C. 2010. Influence of alkali metal sodium doping on the properties of potassium hydrogen phthalate (KHP) crystals. J. Therm. Anal. Calorim. 100:861–865.

[31]Muthu, K.Bhagavannarayan, G and Meenakshisundaram.SP.2012.Growth, crystalline perfection and characterization of Hexaaquanickel(II) dipotassium tetrahydrogen tetra-*o*-phthalate tetrahydrate crystals. Spectrochimica Acta Part A, 92:289– 294.

[32] K. Muthu, G. Bhagavannarayana, S. P. Meenakshisundaram, Solid State Sci., 2012, 14,1355– 1360.

[33] Bairava Ganesh, R. Kannan, V. Meena, K. Rajesh, N.P and Ramasamy, P.2005. Synthesis, growth and characterization of a new nonlinear optical crystal sodium acid phthalate.J.Cryst.Growth. 282:429-433.

[34]G. Ramasamy, S. Meenakshisundaram, 2013. Synthesis and crystal structure of potassium hydrogen phthalate mixed crystal $K_{0.78}Na_{1.22}[C_6H_4(COO)_2]\cdot H_2O$. J. Cryst. Growth, 375:26–31.

[35]Vijila Manonmoni, J. Ramasamy, G. Aditya Prasad, A. Meenakshisundaram, S. P and Amutha, M.2015. Synthesis, growth, structure and characterization of potassium lithium hydrogen phthalate mixed crystals.RSC Advances, 5:42282 – 42289.

[36] Muthu, K.Bagavannarayana, G and Meenakshisundaram, S.P.2012. Synthesis, growth, structure and characterization of nickel(II)-doped hexaaquacobalt(II) dipotassium tetrahydrogen tetra-*o*-phthalate tetrahydrate crystals. Solid state sci., 14, 1355-1360.

[37]Hong-Lei Liu, Hong-Yan Mao, Hong-Yun Zhang, Chen Xu, Qing-An Wu, Gang Li, Yu Zhu, Hong-Wei Hou, 2004. Two novel heterometallacrowns: syntheses and crystal structures of two copper(II) complexes with malonate and *o*-pthalate. polyhedron, 23, 943-948.

[38] Lee, M. H. Yang C. H. and Jan, J. H. 2004. Band-resolved analysis of nonlinear optical properties of crystalline and molecular materials. Phys. Rev. B: Condens. Matter Mater. Phys., 70:235-110.

[39]Rappe, A. M. Rabe, K. M. Kaxiras,E and Joannopoulos, J. D. Optimized Pseudopotentials, Phys. Rev. B: Condens. Matter Mater. Phys., 1990, 41, 1227–1230.

[40]Kleinman, L and Bylander, D. M. 1982. Efficacious Form for Model Pseudopotentials, Phys. Rev. Lett., 48:1425–1428.

[41] Perdew, J. P and Levy, M. 1983. Physical Content of the Exact Kohn-Sham Orbital Energies: Band Gaps and Derivative Discontinuities. Phys. Rev. Lett., 50:1884.

[42] Fangyuan Zhang, Fangfang Zhang, Qun Jing, Shilie Pan, Zhihua Yang and Dianzeng Jia, 2015.Synthesis, Crystal Structureand Properties of the Strontium Vanadate Fluoride $Sr_5(VO_4)_3F$. Z. Anorg. Allg. Chem.,641:1211-1215.

[43]Spackman, M. A and Jayatilaka, D. 2009. Hirshfeld surface analysis. CrystEngComm, 11:19–32.

[44]Spackman, M. A and McKinnon, J. J. 2002. Fingerprinting intermolecular interactions in molecular crystals. *CrystEngComm, 4:378–392*